MicroRNA-16 suppresses the activation of inflammatory macrophages in atherosclerosis by targeting *PDCD4*

XUE LIANG, ZHAO XU, MENG YUAN, YUE ZHANG, BO ZHAO, JUNQIAN WANG, AIXUE ZHANG and GUANGPING LI

Tianjin Key Laboratory of Ionic-Molecular Function of Cardiovascular Disease, Department of Cardiology, Tianjin Institute of Cardiology, Second Hospital of Tianjin Medical University, Tianjin 300211, P.R. China

Received September 30, 2015; Accepted January 27, 2016

DOI: 10.3892/ijmm.2016.2497

Abstract. Programmed cell death 4 (PDCD4) is involved in a number of bioprocesses, such as apoptosis and inflammation. However, its regulatory mechanisms in atherosclerosis remain unclear. In this study, we investigated the role and mechanisms of action of PDCD4 in high-fat diet-induced atherosclerosis in mice and in foam cells (characteristic pathological cells in atherosclerotic lesions) derived from ox-LDL-stimulated macrophages. MicroRNA (miR)-16 was predicted to bind *PDCD4* by bioinformatics analysis. In the mice with atherosclerosis and in the foam cells, PDCD4 protein expression (but not the mRNA expression) was enhanced, while that of miR-16 was reduced. Transfection with miR-16 mimic decreased the activity of a luciferase reporter containing the 3' untranslated region (3'UTR) of *PDCD4* in the macrophage-derived foam cells. Conversely, treatment with miR-16 inhibitor enhanced the luciferase activity. However, by introducing mutations in the predicted binding site located in the 3'UTR of *PDCD4*, the miR-16 mimic and inhibitor were unable to alter the level of PDCD4, suggesting that miR-16 is a direct negative regulator of PDCD4 in atherosclerosis. Furthermore, transfection wtih miR-16 mimic and siRNA targeting *PDCD4* suppressed the secretion and mRNA expression of pro-inflammatory factors, such as interleukin (IL)-6 and tumor necrosis factor-α (TNF-α), whereas it enhanced the secretion and mRNA expression of the anti-inflammatory factor, IL-10. Treatment with miR-16 inhibitor exerted the opposite effects. In addition, the phosphorylation of p38 and extracellular signal-regulated kinase (ERK), and nuclear factor-κB (NF-κB) expression were altered by miR-16. In conclusion, our data demonstrate that the targeting of *PDCD4* by miR-16 may suppress the activation of inflammatory macrophages though mitogen-activated protein kinase (MAPK) and NF-κB signaling in atherosclerosis; thus, PDCD4 may prove to be a potential therapeutic target in the treatment of atherosclerosis.

Correspondence to: Professor Guangping Li, Tianjin Key Laboratory of Ionic-Molecular Function of Cardiovascular Disease, Department of Cardiology, Tianjin Institute of Cardiology, Second Hospital of Tianjin Medical University, 23 Pingjiang Road, Tianjin 300211, P.R. China
E-mail: tjcardiol@126.com

Key words: microRNA-16, programmed cell death 4, atherosclerosis, inflammatory response, mitogen-activated protein kinase and nuclear factor-κB signaling

Introduction

The aging of the population and the increasing incidence of obesity and type 2 diabetes have led to the global burden of atherosclerosis (1), which is a chronic inflammatory disease of the blood vessel wall driven by the subendothelial retention of macrophages (2). The excessive production of oxidized low-density lipoprotein (ox-LDL) in the blood leads to the adequate removal of fats and cholesterol from macrophages, and consequently promotes the formation of multiple atheromatous plaques within the arteries (3). In addition to macrophages, dendritic cells, inflammatory smooth muscle cells, lymphocytes and other inflammatory cells are found in atherosclerotic plaques, indicating the major involvement of immune and inflammatory mechanisms in the pathogenesis of atherosclerosis (4,5). In addition, apoptosis, vascular smooth muscle cell (VSMC) apoptosis in particular, is a critical cellular event responsible for the pathogenesis of atherosclerosis and plaque stability (6).

Programmed cell death 4 (PDCD4) expression is markedly induced by apoptosis and PDCD4 was initially recognized as a tumor suppressor (7). However, the biological functions of PDCD4 in other diseases have been discussed. Apart from tumor cells, PDCD4 has been found to be expressed in cardiac muscle cells and VSMCs (8). In VSMCs, PDCD4 acts as a regulator of apoptosis via activator protein-1 (AP-1) (9), demonstrating the vital role of PDCD4 in cardiovascular disease, particularly in atherosclerosis-related diseases. Furthermore, PDCD4 promotes the inflammatory response by activating nuclear factor-κB (NF-κB) and suppressing interleukin (IL)-10 expression (10,11). These findings underline the potential role of PDCD4 as a novel therapeutic target in the clinical treatment of atherosclerosis.

MicroRNAs (miRNAs or miRs) are small non-encoding RNAs, which play an important role in the fine regulation of multiple physiological processes (12). Both the transcriptional silencing and translational disruption of genes are regulated by miRNAs via direct binding to the 3' or 5' untranslated

region (UTR) (13). To date, a number of atherosclerosis-related miRNAs have been identified, such as miR-33, miR-155, miR-342-5p and miR-126-5p (14,15).

Although PDCD4 has been proven to be a pro-inflammatory protein, the involvement of PDCD4 in atherosclerosis has not been reported until recently. Jiang *et al* found that a deficiency in the *PDCD4* gene had a positive regulatory effect in atherosclerosis by increasing the expression of IL-10 (16). Nevertheless, to the best of our knowledge, miRNAs targeting *PDCD4* in atherosclerosis have not been discovered to date. Hence, in this study, we firstly validated miR-16 as a regulator of *PDCD4* miRNA and examined the alterations in the expression levels of both miR-16 and PDCD4 in high-fat diet induced atherosclerosis in mice and in foam cells derived from ox-LDL-stimulated macrophages. Moreover, the underlying mechanisms were subsequently investigated.

Materials and methods

Reagents, miRNA mimic, inhibitor and antibodies. RPMI-1640 medium, Dulbecco's modified Eagle's medium (DMEM), fetal bovine serum (FBS), penicillin, streptomycin and ox-LDL were purchased from Invitrogen (Shanghai, China). miR-16 mimic, miR-16 inhibitor and siRNA targeting *PDCD4* (*PDCD4* siRNA) were purchased from GenePharma (Shanghai, China), as well as their negative control (NC) oligonucleotide duplex that did not target any gene. Antibodies against p38 (ab7952), phosphorylated (p-)p38 (ab4822), extracellular signal-regulated kinase (ERK; ab180163), p-ERK (ab131438), c-Jun NH2-terminal kinase (JNK; ab199380), p-JNK (ab18680), p65 (ab90532) and PDCD4 (ab79405) were obtained from Abcam (Cambridge, MA, USA).

Prediction of miRNA binding sites. The predicted miRNA binding sites were downloaded from TargetScan 6.2 Mouse (http://www.targetscan.org/mmu_61/).

Animal models of atherosclerosis. *ApoE*$^{-/-}$ mice with a C57BL/6 background were purchased from Beijing University (Beijing, China). The mice used in this study were male, 6-8 weeks old, weighing 20-25 g, and were housed at the Second Hospital of Tianjin Medical University Animal Care Facility (Tianjin, China) under pathogen-free conditions, according to institutional guidelines. All animal study protocols were approved by the Animal Care and Utilization Committee of Tianjin Medical University. At 8 weeks of age, the *ApoE*$^{-/-}$ mice were randomly divided into 2 groups (n=10 in each group). The mice in the control group received a standard diet, while the mice in the model of atherosclerosis group (AS model group) received a high-fat diet (0.25% cholesterol and 15% cocoa butter) for 12 weeks in order to induce the development of atherosclerotic plaques. The animals were then sacrificed by cervical dislocation. The thoracic aorta was immediately harvested after phosphate-buffered saline (PBS) perfusion. Part of the aorta was immersed in 4% paraformaldehyde overnight for immunohistochemical analysis, and the other part of the aorta was stored in liquid nitrogen for the isolation of RNA and protein.

Hematoxylin and eosin (H&E) staining was used to evaluate the atherosclerotic lesions. The mRNA levels of *PDCD4* and miR-16 were measured by reverse transcription-quantitative PCR (RT-qPCR), and the protein epxression levels were measured by western blot analysis and immunohistochemistry.

Macrophage-derived foam cells. The murine macrophage cell line, RAW264.7, was obtained from the American Type Culture Collection (ATCC; Manassas, VA, USA). The cells were maintained in RPMI-1640 (supplemented with 10% FBS, 2 mM L-glutamine, 100 U/ml penicillin G and 100 μg/ml streptomycin) and cultured at 37˚C in a humidified incubator with 5% CO_2. To induce the differentiation of macrophages into foam cells, the RAW264.7 cells were seeded in a 6-well plate and cultured with 50 nM ox-LDL for 24 h.

Transient transfections. RAW264.7 cells were transfected with the indicated concentrations of miR-16 mimic, miR-16 inhibitor or *PDCD4* siRNA (100 nM) using Lipofectamine 2000 according to the manufacturer's instructions (Invitrogen).

Luciferase constructs and reporter gene assays. To obtain recombinant luciferase mRNAs, the DNA segment of the 3'UTR of mouse *PDCD4* mRNA or its mutant, with the changing of the 7 nt binding site for miR-16, was amplified by PCR using modified primers (sense, PDCD4UTR-F-X and antisense, PDCD4UTR-R-N for both the wild-type (WT) and mutant 3'UTRs. As regards the mutated one, 2 additional primers were required to generate the mutant site from the original WT template. One was paired with the aforementioned sense primer, PDCD4UTR-m-F, and the other was used together with the antisense one, PDCD4UTR-m-R. The 2 types of products were then mixed to perform an overlapping PCR experiment and the final product was the expected mutated 3'UTR, digested with *Xho*I and *Not*I. Each of them was then respectively cloned into the vector, siCHECK™-II (Promega, Shanghai, China), downstream of a luciferase CDS. The validity of these constructs was verified by sequencing.

293T cells (ATCC) which were grown in DMEM with high glucose, were used to examine the regulatory effects of miR-16 on PDCD4 mRNA and protein expression. The cells were seeded in 24-well plates and co-transfected with the WT or mutated *PDCD4* 3'UTR combined with dsRNA mimic or inhibitor of miR-16 using Lipofectamine 2000 reagent (Invitrogen). After 48 h of incubation, the cells were harvested and lysates were measured for application in the Luciferase Reporter system (Promega) following the manufacturer's instructions. All the luciferase reporter assays were repeated 3 times within each experiment.

RNA extraction and RT-qPCR. Total RNA from the cultured foam cells and thoracic aorta tissues was isolated using TRIzol reagent (Invitrogen). Reverse transcription was carried out using the M-MLV Reverse Transcription system (Takara, Dalian, China). qPCR was performed using the SYBR-Green PCR kit as described by the manufacture (TransGen, Beijing, China). The primers used for PCR are listed in Table I. Amplification was performed by denaturation at 95˚C for 10 min, followed by 40 cycles of 95˚C for 30 sec, 58˚C for 30 sec and 72˚C for 30 sec. qPCR was carried out on an Applied Biosystems 7500 Fast Real-Time PCR system. The relative mRNA expression levels were normalized to the glyceraldehyde 3-phosphate dehydrogenase (GAPDH) gene according to the $2^{-\Delta\Delta Ct}$ method, and the

Table I. Primers used in this study.

Primers		Sequences (5'→3')
Primers used for plasmid construction		
PDCD4UTR-F-X		AACTCGAGGCACAGCAACTCTTACAGTCTTAGG
PDCD4UTR-R-N		TAGCGGCCGCATTCTTGTAGAACCGGGTTCGT
PDCD4UTR-m-R		CCCATGTTGGCACGACGAGTGGAAATGCTGTGCTT
PDCD4UTR-m-F		AGCATTTCCACTCGTCGTGCCAACATGGGGTTTAG
Reverse transcription PCR		
U6		AACGCTTCACGAATTTGCGT
miR-16		GTCGTATCCAGTGCAGGGTCCGAGGTATTCGCACTGGATACGACCGCCAA
Primers used for RT-qPCR		
GAPDH	Sense	TGCACCACCAACTGCTTAG
	Antisense	GATGCAGGGATGATGTTC
PDCD4	Sense	GTCTTAGGTGTTACCAAGAACAGA
	Antisense	GTTCCTCTTCTGTCCCTCCA
IL-6	Sense	AGTGGCTAAGGACCAAGACC
	Antisense	ACCACAGTGAGGAATGTCCA
TNF-α	Sense	TCAAACCCTGGTATGAGCCC
	Antisense	ACACCCATTCCCTTCACAGA
IL-10	Sense	TGGACTCCAGGACCTAGACA
	Antisense	GTCCCCAATGGAAACAGCTT
TGF-β	Sense	CTGTCCAAACTAAGGCTCGC
	Antisense	TCATAGATGGCGTTGTTGCG
NF-κB	Sense	CCATGCTGATGGAGTACCCT
	Antisense	AGAGAAGTCCATGTCCGCAA
U6	Sense	CTCGCTTCGGCAGCACA
	Antisense	AACGCTTCACGAATTTGCGT
miR-16	Sense	TCGGCGTAGCAGCACGTAAAT
	Universal reverse primer	GTATCCAGTGCAGGGTCCGAGGT

PDCD4, programmed cell death 4; PCR, polymerase chain reaction; IL, interleukin, TNF-α, tumor necrosis factor-α; TGF-β, transforming growth factor-β; NF-κB, nuclear factor-κB.

miRNA expression levels were normalized to U6. All the PCR experiments were carried out in triplicate within each experiment, and the experiments were replicated at least 3 times.

Western blot analysis. Total protein extracts from the cultured foam cell lines and thoracic aorta tissues were prepared in direct lysis buffer [50 mmol/l Tris-HCl (pH 6.8), 100 mmol/l DTT, 2% SDS, 10% glycerol, 1X complete (Roche, Mannheim, Germany) and 0.2% bromophenol blue]. The cells were boiled for 10 min and centrifuged at 13,000 rpm for 5 min. Following 10% sodium dodecyl sulfate-polyacrylamide gel electrophoresis (SDS-PAGE), the proteins were electroblotted onto nitrocellulose membranes (Amersham Biosciences, Piscataway, NJ, USA). The blots were then probed with primary antibodies against p38 (1:5,000), p-p38 (1:1,000), ERK (1:2,000), p-ERK (1:1,000), JNK (1:2,500), p-JNK (1:200), p65 (1:5,000) and PDCD4(1:5000) followed by incubation with the appropriate secondary antibodies, including goat anti-mouse IgG-H&L (HRP) (Abcam; ab136815; 1:10,000) and goat anti-rabbit IgG-H&L (HRP) (Abcam; ab136817; 1:10,000). Protein signals were visualized by using the enhanced chemiluminence (ECL) Western blot detection system (Millipore, Billerica, MA, USA) and quantified by densitometry. All the figures illustrating western blot analyses are representative of at least 3 independent experiments.

Immunohistochemistry. The paraffin-embedded sections (4 ml) were dewaxed and rehydrated in a graded ethanol series. For antigen retrieval, the sections were autoclaved in 0.01 M citrate buffer (pH 6.0) for 30 min, followed by immersion in 3% H_2O_2 methanol for 15 min to block endogenous peroxidase. The sections were then blocked in 15% normal goat serum in phosphate-buffered saline, followed by incubation with polyclonal anti-PDCD4 antibody (1:500) overnight at 4˚C. The sections were then incubated with biotinylated goat anti-rabbit IgG diluted at 1:100 in 15% normal goat serum for 30 min

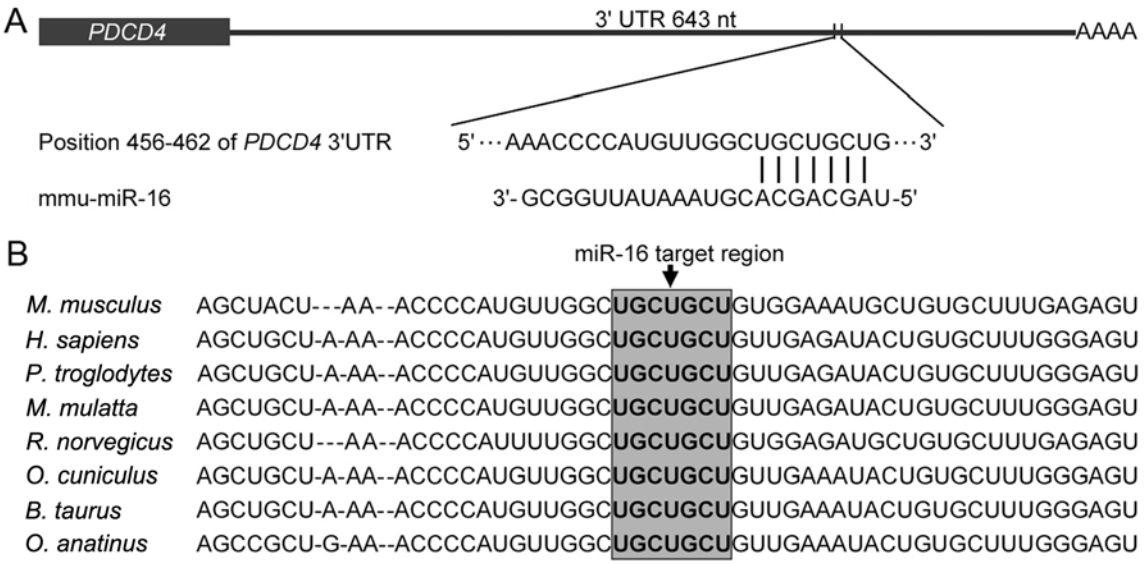

Figure 1. Identification of the binding site of miR-16 in the 3' untranslated region (3'UTR) of programmed cell death 4 (*PDCD4*). (A) Position 456-462 nt in the mouse *PDCD4* 3'UTR was predicted as the binding site of mouse miR-16. (B) Alignment of the *PDCD4* 3'UTR suggested that the miR-16 target sites were highly conserved among different mammalian species.

at room temperature. The standard ABC process was then performed according to the instructions provided with the goat ABC Staining System (Santa Cruz Biotechnology, Inc., Santa Cruz, CA, USA). Diaminobenzidine was used as a chromogen, followed by counterstaining with hematoxylin.

Enzyme-linked immunosorbent assay (ELISA). The secretion of inflammatory factors, including IL-6, tumor necrosis factor-α (TNF-α), IL-10 and transforming growth factor-β (TGF-β) was determined using ELISA. Following transfection and stimulation with ox-LDL for the indicated time periods, the cell supernatants were collected and the amounts of the cytokines in the supernatants were quantified using commercially available ELISA kits (R&D Systems, Minneapolis, MN, USA).

Statistical analysis. All the data are expressed as the means ± SEM and analyzed using SPSS 19.0 software. Differences between 2 groups were analyzed using the Student's t-test, while differences among many groups were analyzed using one-way analysis of variance, followed by Bonferroni's multiple comparison test. Values of $P<0.05$ were considered to represent statistically significant differences.

Results

miR-16 is predicted as a regulator of PDCD4. To determine the regulator of *PDCD4* miRNA, the potential miRNA binding site to the 3'UTR was identified using TargetScan with the 3'UTR of mouse *PDCD4* as the query sequence. As a result, *PDCD4* 3'UTR possessed a nucleotide sequence (456-462 nt) complementary to the miR-16 seed sequence, which indicated a potential binding pattern of miR-16 to *PDCD4* (Fig. 1A). In addition, the nucleotide sequence was highly conserved among different mammalian species (Fig. 1B), demonstrating the conserved function of the miR-16/*PDCD4* regulatory pattern in the evolution of higher animals.

Expression of PDCD4 and miR-16 in a mouse model of atherosclerosis and in foam cells. The association of the expression of PDCD4 and miR-16 with atherosclerosis was assessed using *ApoE*$^{-/-}$ mice fed a high-fat diet (AS model group) compared with mice fed a standard diet (control group). H&E staining of the cross section of the aorta revealed that large plaques were formed after the mice were fed a high-fat diet (indicated by arrows in Fig. 2A), thus indicating that the mouse model of atherosclerosis was successfully developed in the *ApoE*$^{-/-}$ mice. No significant difference in the relative *PDCD4* mRNA expression was observed between the 2 groups ($P>0.05$; Fig. 2B). However, compared with the mice in the control group, the high-fat diet-fed *ApoE*$^{-/-}$ mice exhibited a greater accumulation of PDCD4 protein in the aorta, which was detected by both western blot analysis (Fig. 2C) and immunohistochemistry (Fig. 2D). Conversely, the results of stem-loop RT-qPCR revealed that mature miR-16 was expressed at a markedly lower level in the AS model group than in the control group ($P<0.001$; Fig. 2E).

Additionally, the expression of PDCD4 mRNA and protein and miR-16 was examined in foam cells, characteristic pathological cells in atherosclerotic lesions, which were derived from macrophages stimulated with ox-LDL. Similar to the findings observed in our mouse model of atherosclerosis, the mRNA level of *PDCD4* was not altered ($P>0.05$; Fig. 2F), whereas its protein expression was notably increased in the foam cells (Fig. 2G) and a decreased level of mature miR-16 ($P<0.001$; Fig. 2H) was also observed in the foam cells as compared to the controls (RAW264.7 cells not stimulated with ox-LDL).

PDCD4 is validated as a direct target gene of miR-16. To investigate the role of mature miR-16 in PDCD4 expression, the RAW264.7 cells were transfected with miR-16 mimic or inhibitor. Subsequently, the PDCD4 mRNA and protein levels were detected in the foam cells (ox-LDL-stimulated cells). Neither the miR-16 mimic nor the inhibitor affected the mRNA expression of *PDCD4* ($P=0.413$; Fig. 3A). In addi-

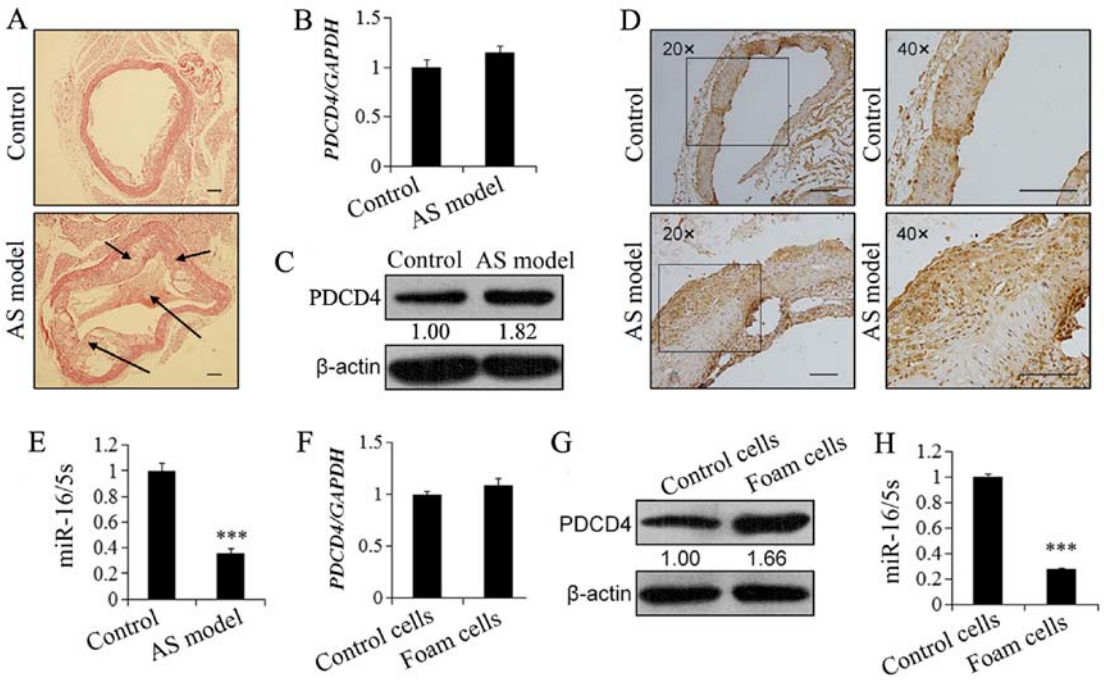

Figure 2. Expression of programmed cell death 4 (PDCD4) and miR-16 in atherosclerosis. (A) Mouse model of atherosclerosis. According to the results of hematoxylin and eosin staining, large plaques (indicated by arrows) were induced by a high-fat diet in the thoracic aorta of the *ApoE*$^{-/-}$ mice, which indicated that the mouse model of atherosclerosis was successfully developed. (B) *PDCD4* mRNA expression in the mice with atherosclerosis was detected by RT-qPCR. (C and D) PDCD4 protein expression in mice with atherosclerosis was detected by (C) western blot analysis and (D) immunohistochemistry. (E) miR-16 expression in mice with atherosclerosis detected by stem-loop RT-qPCR. (F-H) Expression levels of PDCD4 (F) mRNA and (G) protein, as well as (H) miR-16 expression in foam cells derived from oxidized low-density lipoprotein (ox-LDL)-stimulated macrophages. Difference between 2 groups was analyzed using a t-test. ***P<0.001 compared with the control. AS, atherosclerosis.

tion, various concentrations (1, 10 and 100 nM) of miR-16 mimic (Fig. 3B) or inhibitor (Fig. 3C) did not alter *PDCD4* gene expression (P=0.064 and 0.110, respectively). Nevertheless, transfection with miR-16 mimic markedly inhibited the protein expression of PDCD4, while treatment with miR-16 inhibitor led to a 1.6-fold induction in the PDCD4 protein level (Fig. 3D). Moreover, a concentration-dependent influence of the miR-16 mimic and inhibitor on the production of PDCD4 protein was observed (Fig. 3D and F). These findings suggest the post-transcriptional regulation of PDCD4 by miR-16; miR-16 suppresses PDCD4 expression by restraining mRNA translation rather than affecting mRNA stability.

Furthermore, in order to validate the direct regulation of *PDCD4* by miR-16, luciferase reporter plasmids carrying WT or mutated *PDCD4* 3'UTR (Fig. 3G and H) were co-transfected into 293T cells with the miR-16 mimic or inhibitor. The activity of the luciferase reporter in which the WT *PDCD4* 3'UTR was fused to the downstream of the report gene was intensively suppressed by co-transfection with miR-16 mimic (P=0.003), while the activity of the luciferase reporter containing the mutated *PDCD4* 3'UTR was not significantly altered (P>0.05), suggesting that miR-16 suppressed the expression of *PDCD4* by directly binding to the 3'UTR region (Fig. 3I). In addition, no effect of the miR-16 inhibitor was detected on the luciferase reporter carrying the WT or mutated *PDCD4* 3'UTR (P>0.05; Fig. 3I).

Targeting of PDCD4 by miR-16 affects the expression of inflammatory cytokines in atherosclerosis. To address the possible role of miR-16 and PDCD4 in the inflammatory response in atherosclerosis, the RAW264.7 cells were transfected with miR-16 mimic, miR-16 inhibitor or *PDCD4* siRNA and subsequently stimulated with ox-LDL over a 24-h time period to induce the development of foam cells.

The secretion levels of inflammatory factors were then determined by ELISA. The levels of pro-inflammatory cytokines, including IL-6 and TNF-α were enhanced, rapidly reaching peak levels at 6 h and then decreasing (Fig. 4A and B). Compared with the NC oligonucleotide duplex, foam cells harboring the miR-16 mimic or *PDCD4* siRNA exhibited much lower levels of IL-6 and TNF-α (IL-6, P<0.001; TNF-α, P=0.005), while the miR-16 inhibitor promoted the secretion of IL-6 and TNF-α (IL-6, P<0.001; TNF-α, P<0.001). By contrast, the levels of anti-inflammatory cytokines, including IL-10 and TGF-β were suppressed following stimulation with ox-LDL. The level of IL-10 continued to increase during the 24-h time course, while the TGF-β level reached a peak at 12 h. Transfection wtih miR-16 mimic and *PDCD4* siRNA enhanced the secretion of IL-10, whereas treatment with the miR-16 inhibitor exerted the opposite effect (P=0.009; Fig. 4C and D). However, no effects of miR-16 mimic, miR-16 inhibitor or *PDCD4* siRNA on the secretion of TGF-β were detected (P>0.005).

In addition, we determined the mRNA levels of these inflammation factors in foam cells by RT-qPCR. Consistently, transfection with miR-16 mimic and *PDCD4* siRNA exerted an inhibitory effect on the relative mRNA expression levels of IL-6 (P<0.001 and P<0.001, respectively; Fig. 4E) and TNF-α (P=0.003 and P<0.001, respectively; Fig. 4F); however, miR-16 mimic and *PDCD4* siRNA induced the mRNA expres-

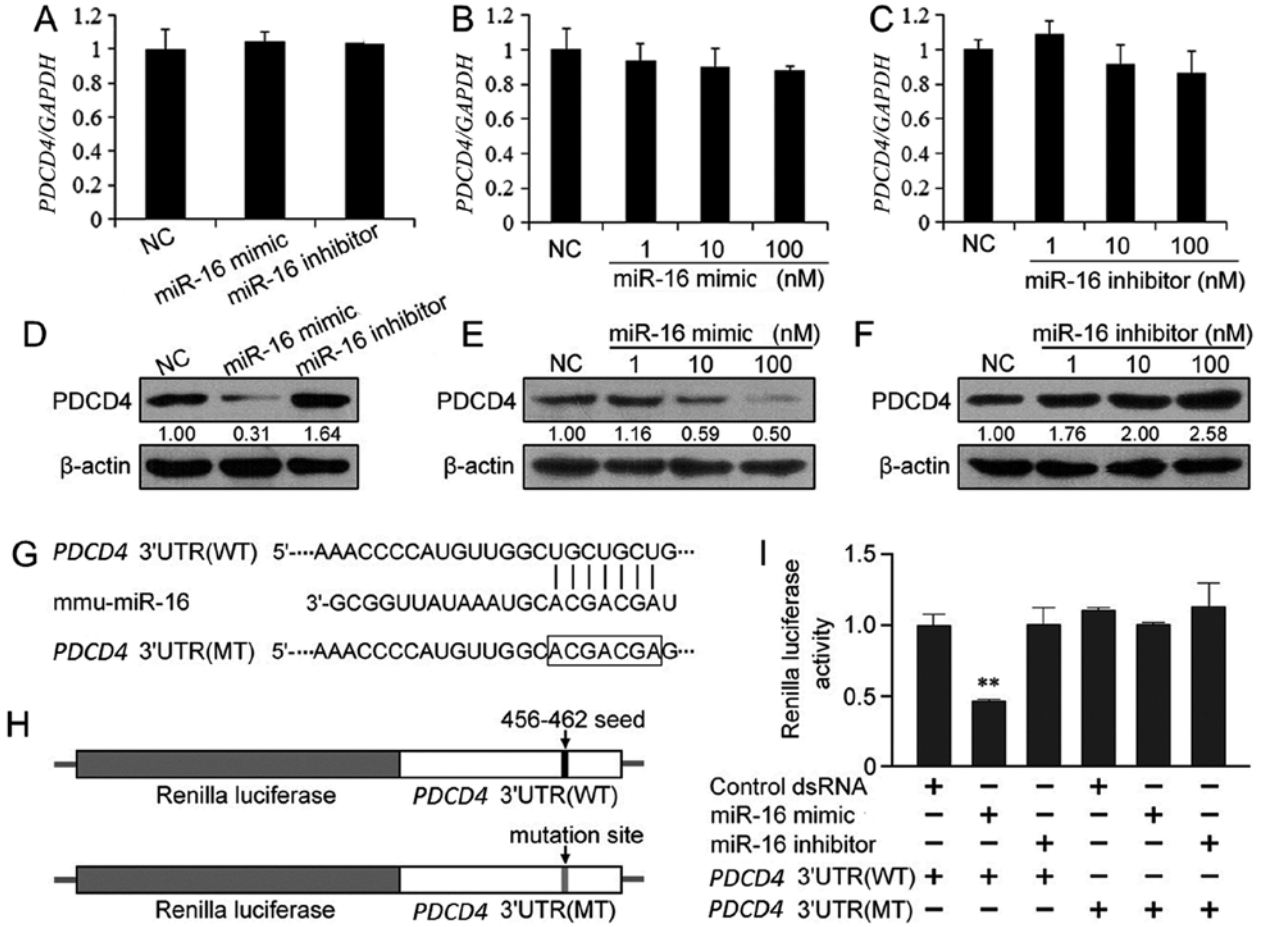

Figure 3. Programmed cell death 4 (*PDCD4*) is the target of miR-16. (A) Effects of miR-16 mimic and inhibitor on the *PDCD4* mRNA expression level in foam cells. (B) Effects of different concentrations of miR-16 mimic on the *PDCD4* mRNA expression level. (C) Effects of different concentrations of miR-16 inhibitor on the *PDCD4* mRNA expression level. (D) Effects of miR-16 mimic and inhibitor on PDCD4 protein expression in foam cells. (E) Effects of different concentrations of miR-16 mimic on PDCD4 protein expression. (F) Effects of different concentrations of miR-16 inhibitor on PDCD4 protein expression. (G) Mutated sequences of *PDCD4* 3' untranslated region (3'UTR). The 7 nt in the miR-16 binding region was changed from UGCUGCU to ACGACGA. (H) A schematic representation of luciferase reporter plasmids carrying wild-type (WT) or mutated (MT) *PDCD4* 3'UTR. (I) Effects of miR-16 mimic and inhibitor on the activity of luciferase reported carrying wild-type or mutated *PDCD4* 3'UTR. Difference between 2 groups was analyzed using a t-test. **P<0.01 compared with the control. NC, negative control (oligonucleotide duplex that did not target any gene).

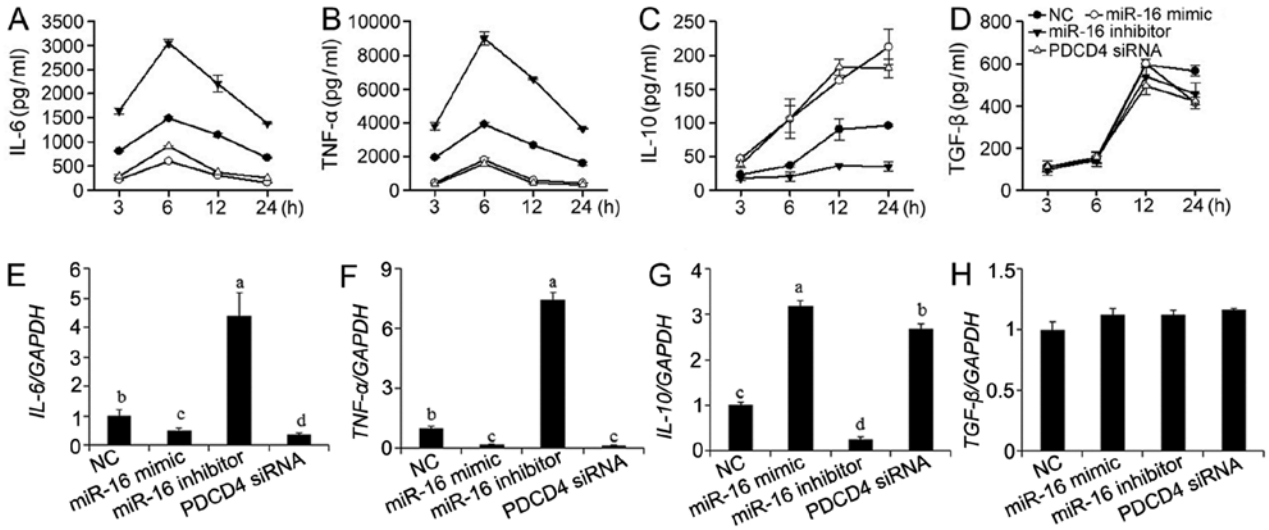

Figure 4. Effects of miR-16 and programmed cell death 4 (PDCD4) expression on the inflammatory response in foam cells. RAW264.7 cells were transfected with miR-16 mimic, miR-16 inhibitor or *PDCD4* siRNA. Foam cells were induced by oxidized low-density lipoprotein (ox-LDL) over a 24-h time course. (A-D) Secretion levels and (E-H) mRNA expression levels of pro- and anti-inflammatory factors including interleukin (IL)-6, tumor necrosis factor-α (TNF-α), IL-10 and transforming growth factor-β1 (TGF-β1). Differences among groups were analyzed by one-way analysis of variance, followed by Bonferroni's multiple comparison test. Values with different letters indicate significant differences with a P-value cut-off of 0.05. NC, negative control (oligonucleotide duplex that did not target any gene).

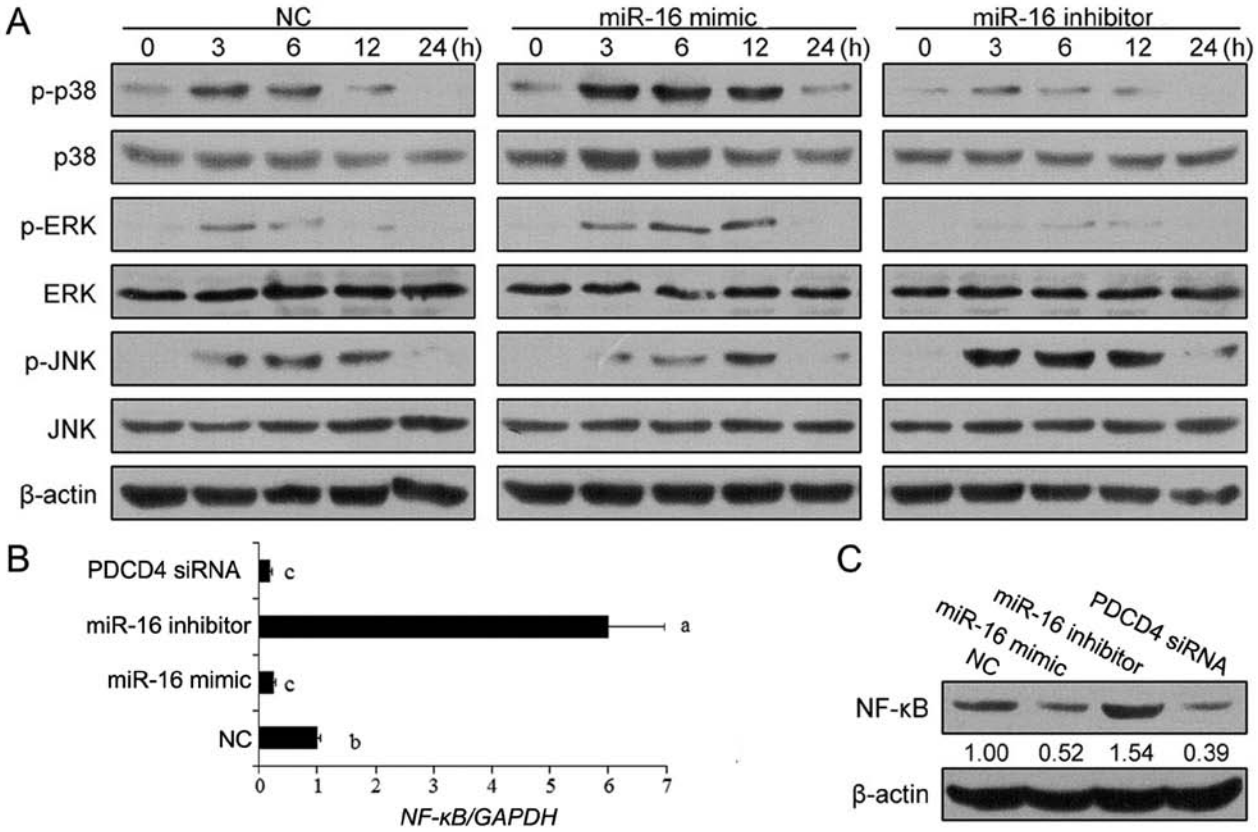

Figure 5. Involvement of the MAPK and NF-κB signaling pathways in miR-16 mediated inflammatory response in foam cells. (A) Effects of miR-16 mimic and inhibitory on p38, ERK and JNK protein expression and phosphorylation during the 24-h oxidized low-density lipoprotein (ox-LDL) treatment time course. (B and C) Effects of miR-16 mimic and inhibitory as well as programmed cell death 4 (*PDCD4*) siRNA on NF-κB (B) mRNA and (C) protein expression in the ox-LDL-treated RAW264.7 cells at the 24-h time point. Differences among groups were analyzed by one-way analysis of variance, followed by Bonferroni's multiple comparison test. Values with different letters indicate significant differences with a P-value cut-off of 0.05. NC, negative control (oligonucleotide duplex that did not target any gene).

sion of IL-10 (P<0.001 and P<0.001, respectively; Fig. 4G). The miR-16 inhibitor increased the IL-6 (P=0.001; Fig. 4E) and TNF-α mRNA levels in the foam cells (P<0.001; Fig. 4F) and decreased IL-10 mRNA expression (P<0.001; Fig. 4G). However, the mRNA level of TGF-β in the foam cells was not significantly altered by miR-16 mimic, miR-16 inhibitor or *PDCD4* siRNA (P>0.05; Fig. 4H).

Targeting of PDCD4 by miR-16 mediates ox-LDL-induced mitogen-activated protein kinase (MAPK) and NF-κB signaling. Considering that MAPK and NF-κB signaling have been implicated in inflammatory cytokine expression (17-19), we thus wished to determine whether these two pathways are involved in the miR-16 induced anti-inflammatory response in atherosclerosis. No significant effects of miR-16 mimic or inhibitor on the protein expression levels of p38, JNK and ERK were observed (Fig. 5A). Nevertheless, the phosphorylation of p38 and ERK was induced, and that of JNK was inhibited by miR-16 mimic. Conversely, the miR-16 inhibitor lowered the phosphorylation level of p38 and ERK, but increased that of JNK (Fig. 5A).

Additionally, NF-κB mRNA expression was prominently suppressed by treatment with miR-16 mimic or siRNA targeting *PDCD4*, but it was increased to approximately 6-fold by the miR-16 inhibitor compared with the NC oligonucleotide duplex (P<0.001; Fig. 5B). Estimates with regard to NF-κB protein expression were consistent with the mRNA results (Fig. 5C).

Discussion

Atherosclerotic vascular disease is the underlying cause of a number of diseases, including claudication, resulting from insufficient blood supply, myocardial infarction, ischemic heart disease and stroke (20). Notably, the two latter diseases are the top two causes of mortality worldwide (21). Thus, the pathogenesis of atherosclerosis is always a critical topic, but it is not yet fully understand. Substantial evidence has suggested that the inflammatory response is triggered in atherosclerosis, which was reflected by the leukocyte recruitment from blood into arterial intima (22,23), and many efforts have been done to investigate the involved molecules (24,25). The pro-inflammatory protein, PDCD4, was recently reported to promote atherosclerosis (16). In the present study, the production of PDCD4 protein was higher in the mice with atherosclerosis and in foam cells derived from ox-LDL-stimulated macrophages, further validating the positive involvement of PDCD4 in the development of atherosclerosis. Additionally, we found that miR-16 was the direct regulatory element of *PDCD4* and played a vital role in atherosclerosis by regulating *PDCD4* and the downstream NF-κB and MAPK pathways.

Initially, miR-16 was well known as a tumor suppressor by inducing apoptosis. Some studies emerged to report the function of miR-16 in immune or inflammatory responses, but yielding inconsistent conclusions. For instance, as previousy demonstrated, in lipopolysaccharide (LPS)-stimulated H69 cells (SV40-transformed human biliary epithelial cells) and U937 cells (human macrophage cell line), the upregulation of miR-16 targets the silencing mediator for retinoid and thyroid hormone receptors (SMRT) and increases the NF-κB-regulated transactivation of IL-8 (26,27). By contrast, during monocyte differentiation into immature and mature dendritic cells, the downregulation of miR-16 has been shown to target the inhibitor of κB (IκB) kinase α (IKKα) and inhibit the activation of NF-κB target genes (28). However, miR-16 promotes the degradation of mRNAs encoding pro-inflammatory factors, such as TNF-α, IL-6 and IL-8 by binding to the AU-rich elements (AREs) in their 3'UTR (29). These findings demonstrate that miR-16 may play different roles in modulating inflammatory factors under different conditions by binding to its different target genes. In this study, we found that the expression of miR-16 was reduced in the mice with atherosclerosis and in foam cells, which indicated the negative role of miR-16 in atherosclerosis. Besides, miR-16 contained a highly conserved UGCUGCU sequence that was complementary to the 3'UTR of *PDCD4*. We did not detect a significant impact of miR-16 mimic or inhibitor on the mRNA expression level of *PDCD4* in the foam cells (derived from RAW264.7 cells stimulated with ox-LDL). Instead, PDCD4 protein production was lowered by miR-16 mimic and increased by miR-16 inhibitor. By using a luciferase construct harboring the sequence of *PDCD4* 3'UTR that was predicted to bind to miR-16, the suppressed protein expression of PDCD4 was detected. By contrast, if mutations were introduced to the sequence of *PDCD4* 3'UTR, miR-16 was unable to affect the production of PDCD4 protein, which implied a translational prevention of PDCD4 by miR-16.

As miR-16 and PDCD4 have been proven to be associated with the inflammatory response (11,27), we examine their effects on inflammatory cytokine expression. Under the stimulation of ox-LDL, macrophages develop into foam cells that modify the production pro-inflammatory factors, such as IL-6 and TNF-α, as well as anti-inflammatory factors, such as IL-10 and TGF-β. Two recent studies demonstrated that IL-10 is suppressed by PDCD4 (11,16). Consistently, in this study, we found that the transfection of cells with miR-16 mimic or *PDCD4* siRNA promoted the release and mRNA expression of IL-10, while miR-16 inhibitor exerted the opposite effect. However, the effect of PDCD4 on other inflammatory cytokines is debatable. For instance, the expression of IL-6 has been shown to be blocked by *PDCD4* deficiency in the LPS-induced inflammatory response (11), while in another study, IL-6, TNF-α and TGF-β were not significantly altered between ox-LDL-treated macrophages from *PDCD4*$^{-/-}$*ApoE*$^{-/-}$ and *PDCD4*$^{+/+}$*ApoE*$^{-/-}$ mice (16). In this study, transfection of the RAW264.7 cells with miR-16 inhibitor, miR-16 mimic or *PDCD4* siRNA was used. Following stimulation with ox-LDL for various periods of time, miR-16 mimic inhibited the release and mRNA expression of IL-6 and TNF-α, which may be partly due to the direct regulation of miR-16 on their mRNA degradation (29). Besides, we also detected similar results in foam cells, which was inconsistent with the previous study (16). Although different cell sources and ox-LDL concentrations were employed, these incongruous results cannot be well explained and require further investigation.

The MAPK pathway has a critical function in inflammatory diseases, including atherosclerosis (30). It has been reported that MAPK signaling contributes to the regulation of pro- and anti-inflammatory cytokines (TNF-α and IL-10) in macrophages by the activation of p38 and JNK (31). Jiang *et al* found that the induction of IL-10 in mice deficient in *PDCD4* was blocked by the inhibition of the p38/ERK-c-Maf pathway (16) Consistently, in the present study, miR-16 markedly increased the phosphorylation of p38 and ERK, suggesting that the p38/ERK-c-Maf pathway may be involved in the miR-16 mediated inflammatory response in atherosclerosis. Besides, miR-16 suppressed the phosphorylation of JNK. JNK MAPK phosphorylation has been well-documented to activate NF-κB, which mediates vascular inflammation in the initiation and progression of atherosclerosis (1). Several miRNAs block or promote the activity or expression of NF-κB in atherosclerosis, such as miR-21 (32), miR-181b (33) and miR-29b (34). In this study, we also presented evidence that miR-16 inhibits the mRNA and protein expression of NF-κB in foam cells derived from ox-LDL-stimulated macrophages. The NF-κB pathway in endothelial cells leads to the elevated expression of downstream pro-inflammatory cytokines, including IL-6 and TNF-α (35). Hence, we assumed that our findings with regard to the effects of miR-16 and *PDCD4* on IL-6 and TNF-α are a result of the altered phosphorylation levels of JNK and MAPK, as well as the expression level of NF-κB.

In conclusion, the findings of the present study suggest that miR-16 directly targets *PDCD4* to suppress the activation of inflammatory macrophages in atherosclerosis via the MAPK and NF-κB pathways and downstream inflammatory cytokines. Four potential mechanisms of miR-16 are indicated in atherosclerosis: i) the decreased expression of miR-16 upregulates the mRNA level of pro-inflammatory factors by binding to the AREs in their 3'UTR; the decreased expression of miR-16 weakens its translational prevention role on PDCD4, which ii) reduces the IL-10 level by inhibiting the p38/ERK-c-Maf pathway and enhancing the expression of IL-6 and TNF-α by iii) activating NF-κB by JNK MAPK or iv) increasing NF-κB expression. In addition to PDCD4, miR-16 may be used as a potential therapeutic target in the treatment of atherosclerosis.

Acknowledgements

The present study was approved by the Tianjin Municipal Science and technology project (no. 13ZCZDSY01400), the Specialized Research Fund for the Doctoral Program of Higher Education of China (no. 20121202110004), as well as the China Postdoctoral Science Foundation funded project (no. 2015M571272).

References

1. Tabas I, García-Cardeña G and Owens GK: Recent insights into the cellular biology of atherosclerosis. J Cell Biol 209: 13-22, 2015.
2. Ross R: Atherosclerosis - an inflammatory disease. N Engl J Med 340: 115-126, 1999.

3. Kataoka H, Kume N, Miyamoto S, Minami M, Morimoto M, Hayashida K, Hashimoto N and Kita T: Oxidized LDL modulates Bax/Bcl-2 through the lectinlike Ox-LDL receptor-1 in vascular smooth muscle cells. Arterioscler Thromb Vasc Biol 21: 955-960, 2001.
4. Galkina E and Ley K: Immune and inflammatory mechanisms of atherosclerosis (*). Annu Rev Immunol 27: 165-197, 2009.
5. Legein B, Temmerman L, Biessen EA and Lutgens E: Inflammation and immune system interactions in atherosclerosis. Cell Mol Life Sci 70: 3847-3869, 2013.
6. Clarke M and Bennett M: The emerging role of vascular smooth muscle cell apoptosis in atherosclerosis and plaque stability. Am J Nephrol 26: 531-535, 2006.
7. Lankat-Buttgereit B and Göke R: The tumour suppressor Pdcd4: recent advances in the elucidation of function and regulation. Biol Cell 101: 309-317, 2009.
8. Cheng Y, Liu X, Zhang S, Lin Y, Yang J and Zhang C: MicroRNA-21 protects against the H(2)O(2)-induced injury on cardiac myocytes via its target gene PDCD4. J Mol Cell Cardiol 47: 5-14, 2009.
9. Liu X, Cheng Y, Yang J, Krall TJ, Huo Y and Zhang C: An essential role of PDCD4 in vascular smooth muscle cell apoptosis and proliferation: Implications for vascular disease. Am J Physiol Cell Physiol 298: C1481-C1488, 2010.
10. Merline R, Moreth K, Beckmann J, Nastase MV, Zeng-Brouwers J, Tralhão JG, Lemarchand P, Pfeilschifter J, Schaefer RM, Iozzo RV and Schaefer L: Signaling by the matrix proteoglycan decorin controls inflammation and cancer through PDCD4 and MicroRNA-21. Sci Signal 4: ra75-ra75, 2011.
11. Sheedy FJ, Palsson-McDermott E, Hennessy EJ, Martin C, O'Leary JJ, Ruan Q, Johnson DS, Chen Y and O'Neill LA: Negative regulation of TLR4 via targeting of the proinflammatory tumor suppressor PDCD4 by the microRNA miR-21. Nat Immunol 11: 141-147, 2010.
12. He L and Hannon GJ: MicroRNAs: Small RNAs with a big role in gene regulation. Nat Rev Genet 5: 522-531, 2004.
13. El Gazzar M, Church A, Liu T and McCall CE: MicroRNA-146a regulates both transcription silencing and translation disruption of TNF-α during TLR4-induced gene reprogramming. J Leukoc Biol 90: 509-519, 2011.
14. Nazari-Jahantigh M, Wei Y, Noels H, Akhtar S, Zhou Z, Koenen RR, Heyll K, Gremse F, Kiessling F, Grommes J, *et al*: MicroRNA-155 promotes atherosclerosis by repressing Bcl6 in macrophages. J Clin Invest 122: 4190-4202, 2012.
15. Horie T, Baba O, Kuwabara Y, Chujo Y, Watanabe S, Kinoshita M, Horiguchi M, Nakamura T, Chonabayashi K, Hishizawa M, *et al*: MicroRNA-33 deficiency reduces the progression of atherosclerotic plaque in ApoE$^{-/-}$ mice. J Am Heart Assoc 1: e003376, 2012.
16. Jiang Y, Gao Q, Wang L, Guo C, Zhu F, Wang B, Wang Q, Gao F, Chen Y and Zhang L: Deficiency of programmed cell death 4 results in increased IL-10 expression by macrophages and thereby attenuates atherosclerosis in hyperlipidemic mice. Cell Mol Immunol: Jul 13, 2015 (Epub ahead of print). doi: 10.1038/cmi.2015.47.
17. Cho JW, Lee KS and Kim CW: Curcumin attenuates the expression of IL-1β, IL-6, and TNF-α as well as cyclin E in TNF-α-treated HaCaT cells; NF-κB and MAPKs as potential upstream targets. Int J Mol Med 19: 469-474, 2007.
18. Johnson GL and Lapadat R: Mitogen-activated protein kinase pathways mediated by ERK, JNK, and p38 protein kinases. Science 298: 1911-1912, 2002.
19. Tak PP and Firestein GS: NF-kappaB: a key role in inflammatory diseases. J Clin Invest 107: 7-11, 2001.
20. Lusis AJ: Atherosclerosis. Nature 407: 233-241, 2000.
21. Organization WH: The top 10 causes of death. 2014. Available at: http://wwwwhoint/mediacentre/factsheets/fs310/en/. Accessed March 26, 2015.
22. Cybulsky MI, Won D and Haidari M: Leukocyte recruitment to atherosclerotic lesions. Can J Cardiol 20 (Suppl B): 24B-28B, 2004.
23. Libby P, Ridker PM and Maseri A: Inflammation and atherosclerosis. Circulation 105: 1135-1143, 2002.
24. Eriksson EE: Mechanisms of leukocyte recruitment to atherosclerotic lesions: future prospects. Curr Opin Lipidol 15: 553-558, 2004.
25. Yang L, Chu Y, Wang Y, Zhao X, Xu W, Zhang P, Liu X, Dong S, He W and Gao C: siRNA-mediated silencing of Wnt5a regulates inflammatory responses in atherosclerosis through the MAPK/NF-κB pathways. Int J Mol Med 34: 1147-1152, 2014.
26. Zhou R, Hu G, Gong AY and Chen XM: Binding of NF-kappaB p65 subunit to the promoter elements is involved in LPS-induced transactivation of miRNA genes in human biliary epithelial cells. Nucleic Acids Res 38: 3222-3232, 2010.
27. Zhou R, Li X, Hu G, Gong AY, Drescher KM and Chen XM: miR-16 targets transcriptional corepressor SMRT and modulates NF-kappaB-regulated transactivation of interleukin-8 gene. PLoS One 7: e30772, 2012.
28. Li T, Morgan MJ, Choksi S, Zhang Y, Kim YS and Liu ZG: MicroRNAs modulate the noncanonical transcription factor NF-kappaB pathway by regulating expression of the kinase IKKalpha during macrophage differentiation. Nat Immunol 11: 799-805, 2010.
29. Jing Q, Huang S, Guth S, Zarubin T, Motoyama A, Chen J, Di Padova F, Lin SC, Gram H and Han J: Involvement of microRNA in AU-rich element-mediated mRNA instability. Cell 120: 623-634, 2005.
30. Seimon TA, Wang Y, Han S, Senokuchi T, Schrijvers DM, Kuriakose G, Tall AR and Tabas IA: Macrophage deficiency of p38alpha MAPK promotes apoptosis and plaque necrosis in advanced atherosclerotic lesions in mice. J Clin Invest 119: 886-898, 2009.
31. Chi H, Barry SP, Roth RJ, Wu JJ, Jones EA, Bennett AM and Flavell RA: Dynamic regulation of pro- and anti-inflammatory cytokines by MAPK phosphatase 1 (MKP-1) in innate immune responses. Proc Natl Acad Sci USA 103: 2274-2279, 2006.
32. Asangani IA, Rasheed SA, Nikolova DA, Leupold JH, Colburn NH, Post S and Allgayer H: MicroRNA-21 (miR-21) post-transcriptionally downregulates tumor suppressor Pdcd4 and stimulates invasion, intravasation and metastasis in colorectal cancer. Oncogene 27: 2128-2136, 2008.
33. Sun X, He S, Wara AK, Icli B, Shvartz E, Tesmenitsky Y, Belkin N, Li D, Blackwell TS, Sukhova GK, *et al*: Systemic delivery of microRNA-181b inhibits nuclear factor-κB activation, vascular inflammation, and atherosclerosis in apolipoprotein E-deficient mice. Circ Res 114: 32-40, 2014.
34. Zhu HQ, li Q, Dong LY, Zhou Q, Wang H and Wang Y: MicroRNA-29b promotes high-fat diet-stimulated endothelial permeability and apoptosis in apoE knock-out mice by down-regulating MT1 expression. Int J Cardiol 176: 764-770, 2014.
35. Kempe S, Kestler H, Lasar A and Wirth T: NF-kappaB controls the global pro-inflammatory response in endothelial cells: Evidence for the regulation of a pro-atherogenic program. Nucleic Acids Res 33: 5308-5319, 2005.